

Article

Spatiotemporal Characteristics and Influencing Factors of Summer Heatwaves in Hexi Oasis during 1962–2020

Juan Lu ^{1,2,3}, Puxing Liu ^{1,2,*} and Huiyu Wang ³¹ College of Geography and Environmental Science, Northwest Normal University, Lanzhou 730070, China² Key Laboratory of Resource Environment and Sustainable Development of Oasis, Lanzhou 730030, China³ College of Geology and Jewelry, Lanzhou Resources & Environment Voc-Tech University, Lanzhou 730021, China

* Correspondence: lpx401@126.com

Abstract: Based on the daily gridded ($0.5^\circ \times 0.5^\circ$) maximum temperature data during 1962–2020, the spatiotemporal characteristics of heatwaves in Hexi Oasis, Gansu Province, China and their influencing factors are investigated. The results showed that for the last 59 years, the overall trends of high-temperature heatwaves in Hexi Oasis were prolonged duration (0.276 d/10a), increased frequency (0.007 times/10a), and decreased intensity ($-0.072^\circ\text{C}/10\text{a}$). In terms of spatial variation, there was a gradually decreasing trend from northwest to southeast for both the duration and frequency of heatwaves. In the contrary, heatwaves with higher intensity were mainly distributed over the southeastern and central parts of Hexi Oasis. The Mann–Kendall (M-K) analysis demonstrated that the mutation years of the duration and intensity of heatwaves are 2009 and 1992, respectively, while the frequency remained nearly constant for the last 59a. In addition, the cycles for the duration (2.6a and 7.2a), frequency (2.8a and 7.6a), and intensity (2.6a) of heatwaves agree well with those of atmospheric circulation and El Niño events, indicating that the above events have a great impact on the heatwaves. The influencing factors analysis implies that the heatwaves are mainly influenced by Asian zone polar vortex area index (APVAI), East Asia major trough (EAT), Qinghai-Tibetan Plateau index (TPI), and carbon dioxide emissions (CDE). Additionally, it is concluded that the intensity of heatwaves was negatively correlated with the size of the subtropical high-pressure area in the western Pacific Ocean.



Citation: Lu, J.; Liu, P.; Wang, H. Spatiotemporal Characteristics and Influencing Factors of Summer Heatwaves in Hexi Oasis during 1962–2020. *Atmosphere* **2023**, *14*, 119. <https://doi.org/10.3390/atmos14010119>

Academic Editor: Wei Zhang

Received: 8 December 2022

Revised: 27 December 2022

Accepted: 30 December 2022

Published: 5 January 2023



Copyright: © 2023 by the authors. Licensee MDPI, Basel, Switzerland. This article is an open access article distributed under the terms and conditions of the Creative Commons Attribution (CC BY) license (<https://creativecommons.org/licenses/by/4.0/>).

Keywords: high-temperature heatwaves; Hexi Oasis; spatiotemporal variations; influencing factor; extreme climate

1. Introduction

Global warming has been intensifying since the industrial revolution [1], which causes the frequent occurrence of extreme climate events, shrinking cryosphere, rising sea level, and decreasing biodiversity, and as a result strongly affects the natural ecosystem and the sustainable development of human socioeconomics [2]. Specifically, the extreme climate events have great effects on food security, natural disasters, and many other aspects [3,4], among which the high-temperature heatwaves are considered as one of the most serious events and are more prominent in response to global warming [5]. Heatwaves are defined as continuous high-temperature weather conditions lasting for several days [6]. Thus, it is of vital importance to study the spatiotemporal change characteristics and influencing factors of heatwaves.

Numerous studies have shown that the duration, frequency, and intensity of global heatwaves increased significantly over the past few decades, especially under the context of global warming [1]. Even during periods of global warming stagnation, extreme warm events continue to increase, with their frequency increasing twofold in the past century [7]. In 2003, Europe experienced the most intense heatwave on record, with average summer temperatures rising by $4\text{--}5.5^\circ\text{C}$ compared to 1962–1999, which directly led to 15,000 deaths

and economic losses of more than 10 billion euros in France [8,9]. Habeeb et al. [10] reported that the duration, frequency, and intensity of heatwaves in the United States have continued to increase in the last 50 years. Similarly, Russia experienced an unprecedented heatwave event, with more than 54,000 people falling ill [11]. The occurrence of heatwaves in China also showed an overall increasing trend for the last several decades, which is basically synchronized with those of the globe. Based on the temperature data of 719 meteorological stations in China, Jia et al. [12] concluded that the strong heatwaves were mainly distributed in southern and southwestern China, and the weak heatwaves were concentrated in northwestern China. Shen [13] concluded that the national heatwave index of China decreased during the 1960s–1980s and increased after 1990s, and the heatwaves with high-intensity occurred frequently after 1998, especially south of the Yangtze River region. Many researchers have already proved that the heatwaves would cause immense stress on human society and the natural environments. For example, in 2017, most of China suffered from an intense heatwave that resulted in a disaster area of crops of approximately $5836.1 \times 10^3 \text{ hm}^2$, among which the area with crop failure is up to 6%, with an economic loss of RMB 16.16 billion [14]. Studies have shown that heatwave-related deaths in China are characterized by rapid growth and nonlinear spatial–temporal evolution in the last 40 years, and people aged over 75 have been significantly more affected by heatwaves than other age groups [2]. Furthermore, the study conducted by Yang et al. [15] also showed that the incidence of coronary heart disease, stroke, and respiratory disease increased significantly with the prolongation of heatwave.

Although there are many studies about heatwaves in China contributing to positive progress, the study areas are mainly focused on the regional and national scales [12,13,16]. Under the background of global warming, the warming of northwest China is more pronounced and sensitive to climate changes [17]. However, there is a lack of studies on the characteristics of heatwaves in this region. Hexi Oasis with a fragile ecological environment, representing a large temperate arid and semi-arid region in northwest China, would suffer more serious threats from extreme climate events, such as heatwaves and droughts [18,19]. Meanwhile, Hexi Oasis is an important crop production area in Gansu province and even in the northwest China. Thus, it is valuable to study the extreme climate events in Hexi Oasis to reduce the natural hazards in northwestern China. However, although a lot of fruitful studies have been performed on extreme climate events, such as extreme heat in Hexi Oasis, few studies are conducted on heatwaves. Therefore, in order to clarify the effects of heatwaves on the human health and crop production in northwest China, the characteristics of heatwaves in Hexi Oasis as a model were studied in the present work. By using the Mann–Kendall and wavelet power spectrum analyses, the spatiotemporal characteristics of heatwaves in Hexi Oasis and their influencing factors were investigated with the daily maximum temperature grid point data from 1962 to 2020, providing scientific basis for Hexi Oasis to cope with an extreme climate and contributing to the restoration and reconstruction of the ecological environment in the arid zone.

2. Data and Method

2.1. Study Area

Hexi Oasis is located at $35^{\circ}36' \text{ N}$ – $42^{\circ}19' \text{ N}$, $85^{\circ}02' \text{ E}$ – $114^{\circ}25' \text{ E}$, which is in the second steppe of China's topography. The main landform types of Hexi Oasis are large pre-mountain flood fans and impact plains with high altitude (Figure 1). This area is a temperate continental arid climate with long sunshine hours and abundant light and heat resources. The multi-year average temperature, precipitation, evaporation, wind speed, and sunshine hours are $4\text{--}10 \text{ }^{\circ}\text{C}$, $9.5\text{--}592.8 \text{ mm}$, $1650\text{--}3500 \text{ mm}$, $2.0\text{--}4.2 \text{ m/s}$, and $2800\text{--}3300 \text{ h}$, respectively. The climate of Hexi Oasis varies sharply between hot and cold seasons, with strong winds and sandy conditions. The annual precipitation gradually decreases from southeast to northwest, and the dryness index gradually increases. From west to east, there are 3 independent endorheic river systems, namely Shule River, Hei River, and Shiyang River, and 15 rivers with annual runoff above $1 \times 10^8 \text{ m}^3$. The main soil types in Hexi Oasis

include brown desert soil, gray, brown desert soil, gray desert soil, light brown calcium soil, gray calcium soil, aeolian sandy soil, meadow soil, and other arid soil types. The irrigated agricultural area in Hexi Oasis has a long history and is one of the important agricultural areas in Gansu Province, mainly planting spring wheat, corn, potatoes, caraway, barley, and other crop varieties. In order to prevent the sand, heatwaves, and dry hot wind invasion, Calligonum, Camellia, Tamarix, Populus euphratica, Hippophae rhamnoides, and Caragana korshinskii were adopted in the oasis area to create a windbreak forest belt, which has had a remarkable effect [20,21].

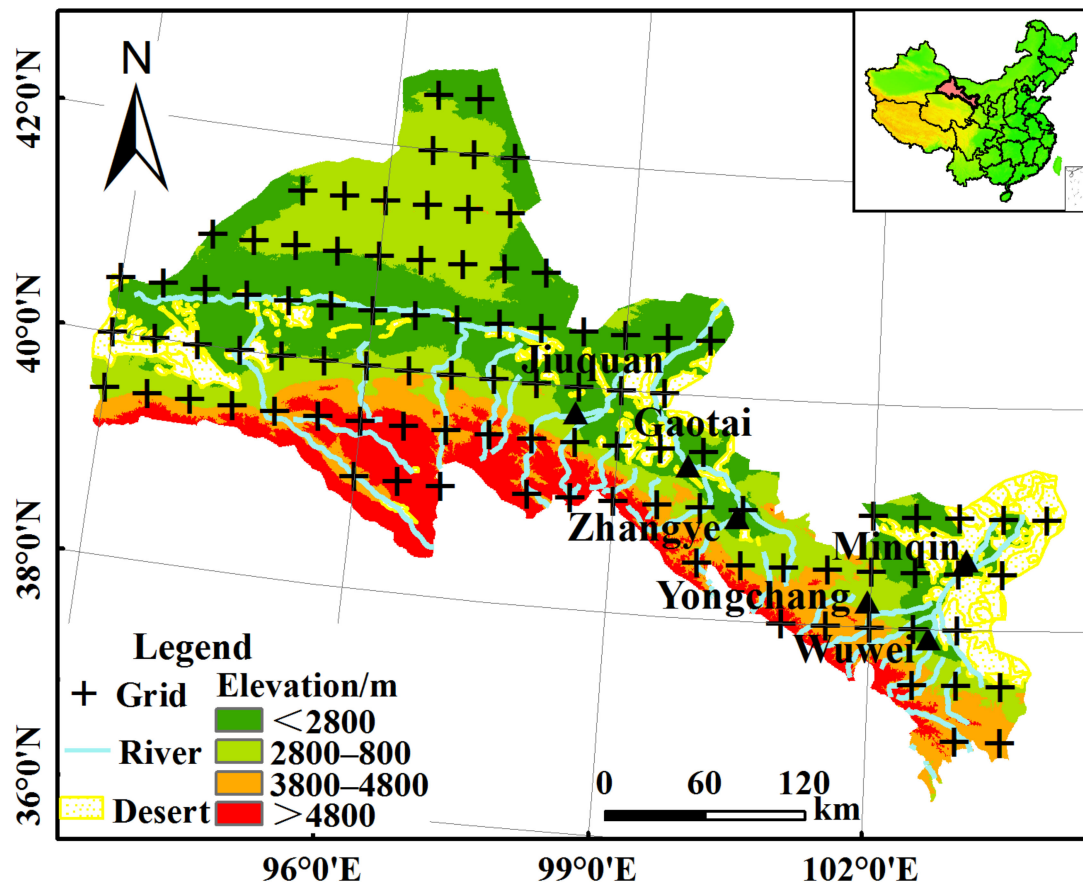


Figure 1. Distribution of the meteorological grids in Hexi Oasis.

2.2. Data Sources

The meteorological data used in this study were obtained from the surface daily temperature maximum grid data with a resolution of $0.5^\circ \times 0.5^\circ$ from 1962 to 2020 provided by China Meteorological Data Network "<http://data.cma.cn/> (accessed on 1 January 2023)". Circulation characteristics indices were the Asian Polar Vortex Area Index (APVAI), Asian Polar Vortex Intensity Index (APVII), East Asian Trough Intensity (EAT), Tibetan Plateau Index (TPI), and Arctic Oscillation Index (AO) provided by the National Climate Center. Average annual carbon dioxide emissions (CDE) (1970–2018) were obtained from the World Bank's Development Indicators Database (WDI) "<http://data.worldbank.org/> (accessed on 1 January 2023)". The Western Pacific Sub-High Area Index (WPSHA), Western Pacific Sub-High Intensity Index (WPSHI), Western Pacific Sub-High Ridge Position Index (WPSHRPI), and Western Pacific Sub-High Northern Boundary Position Index (WPSHNBP) are from the National Climate Center's 130 climate system dataset, and the El Niño dataset is from the Pacific Marine Environment Laboratory "<https://www.Pmel.noaa.gov/> (accessed on 1 January 2023)". All the time length of the above data are from 1962 to 2020 (June to September). Data from 1961 are incomplete, and thus they have been excluded to ensure the accuracy of the study.

2.3. Research Methods

Generally, the critical value method and the relative threshold method are used to define the high-temperature heatwaves, wherein the former the high-temperature heatwaves are defined by exceeding a certain temperature threshold; and in the latter by continuously passing the 90th or 95th percentile of the daily maximum temperature. The physical geography varies greatly within the Hexi Oasis, which makes it is difficult to eliminate different climatic and topographical differences by using the critical value method. Thus, the relative threshold method proposed by Hobday et al. [5] was adopted in the present study to define the high-temperature heatwave event, which usually uses 30 years as the climate reference period to calculate high-temperature days (in this work, 1985–2015 was used as the climate reference period) and define the high-temperature heatwave event [22].

For an arbitrary day (h), rank the highest temperatures for the 5 days before and after the climate reference period, and take the 90th quantile of the highest temperature in the 11 days range as the threshold of the high-temperature day, above which the day can be defined as a high-temperature day.

$$T_{90}(h) = P_{90}(X) \quad (1)$$

where $T_{90}(h)$ is the h -day maximum temperature threshold temperature; P_{90} is the 90th quantile; for a given day h , the 90th quantile of the daily maximum temperature between $h - 5$ and $h + 5$ and within the reference period 1986–2015, a total of 11×30 d, is the daily high-temperature threshold. A high-temperature day lasting more than 5 days is a heatwave event, and heatwaves separated by ≤ 2 days can be considered as one heatwave event. The number of heatwaves per year and their days were defined as the frequency and duration of heatwave. The average difference between the daily maximum temperature during a heatwave event and the average daily maximum temperature during the climate reference period is used to definite the intensity of a heatwave and is calculated as follows:

$$I_{mean} = \overline{T(t)} - T_m(h) \quad (2)$$

$$T_m(h) = \sum_{y=y_s}^{y_e} \sum_{d=h-5}^{h+5} \frac{T(y,d)}{11(y_e-y_s+1)} \quad (3)$$

where I_{mean} is the average intensity of high-temperature heatwave, T is the maximum temperature, t is the high-temperature day ($t_s \leq t \leq t_e$, t_s is the start date of the high-temperature heatwave, t_e is the end date), and $T_m(h)$ indicates the average daily maximum temperature of the climate reference period, $h(t_s) \leq h \leq h(t_e)$.

3. Results and Discussion

3.1. Temporal and Spatial Characteristics of the Recent 59a High-Temperature Heatwave in Hexi Oasis

For the last 59a, the overall trend of high-temperature heatwaves in Hexi Oasis has shown an extended duration, increased frequency, and reduced intensity. The average duration of high-temperature heatwaves was 6.80 days, with the longest duration of 13.7 days (at 1999 and 2019), followed by 12.4 days (2016) and 10.7 days (1986), and the shortest duration of three days (1973). In terms of trend, the rate of increase in the duration of heatwave was 0.276 d/10a ($p < 0.1$). According to Yao et al. [23], the tendency change of temperature in Hexi Oasis from 1961–2018 is 0.364 °C/10a. There is a significant decreasing trend in the duration of heatwaves from 1981 to 1990, while an increasing trend was observed in the range of 1991–2000 (as shown in Figure 2a and Table 1). In addition, in Table 1, one can observe that there are negative values of duration which represent an overall decreasing trend of heatwave events in the 1980s compared to that of other interdecadal periods. This may be due to the relatively high activity of cold air during this period [24]. From Figure 2b, the interdecadal variation in frequency was generally consistent with that in duration of heatwave, with a slight increasing trend of

0.007 times/10a and a mean value of 1.2 times. The highest frequency of heatwaves was two times a year in 2019, followed by 1.8 times in both 1986 and 1999 (Figure 2b, Table 1). The intensity of heatwaves decreased in a trend of $-0.072\text{ }^{\circ}\text{C}/10\text{a}$ with an average intensity of $5.6\text{ }^{\circ}\text{C}$. The maximum intensity of heatwave was $6.8\text{ }^{\circ}\text{C}$ in 1998, while the minimum intensity was $4.2\text{ }^{\circ}\text{C}$ in 2015. Regarding the interdecadal variations, all the tendency rates of intensity are positive except for the 1990s, and the most obvious increase occurred in the 1970s with a maximum rate of change of $2.02\text{ }^{\circ}\text{C}/10\text{a}$ (Figure 2c, Table 1). For the 1990s, there is the increasing change of heatwaves in Hexi Oasis, this is consistent with the results Ye et al., which concluded that since the 1990s, the duration and intensity of summer heat waves in China have increased significantly, mainly related to global warming, and secondly, that the urban heat island effect has become more pronounced due to accelerated urbanization, reduced vegetation cover, expanded city size, and increased population density in China. This has undoubtedly intensified the extreme heat of summer heat [25]. In addition, the total number of days, average number of days, and average frequency of heatwaves in Hexi Oasis all reached maximum values in 2019. This is because 2019 was the hottest summer on record in the Northern Hemisphere with an average temperature of $1.66\text{ }^{\circ}\text{C}$ higher than usual [17,24,26].

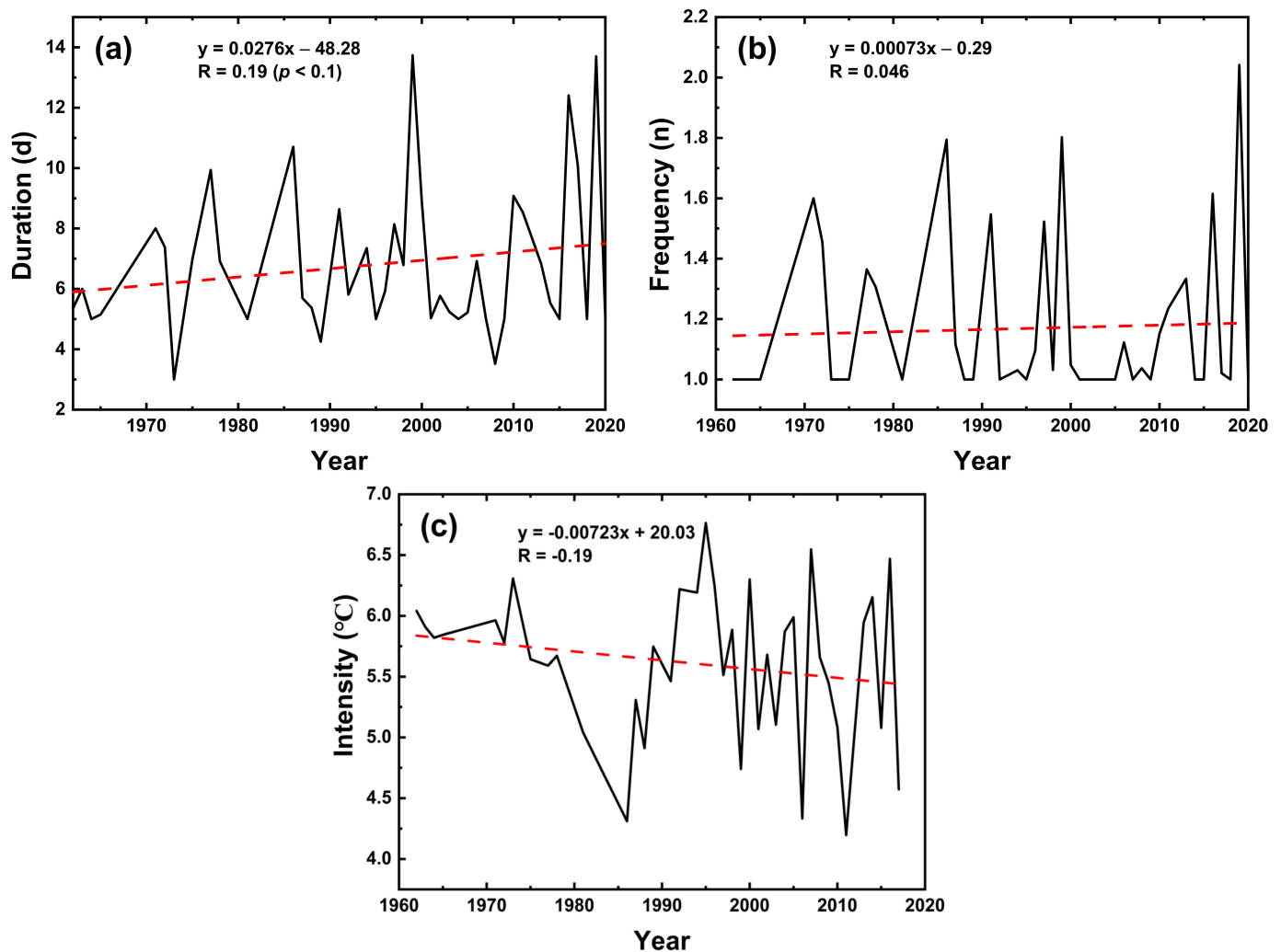


Figure 2. Temporal variation characteristics of duration (a), frequency (b) and intensity (c) of high-temperature heatwaves in Hexi Oasis from 1962 to 2020. The black lines are annual average temperatures and the red dotted lines are trend-lines.

Table 1. Interdecadal trends in high-temperature heatwaves in Hexi Oasis.

Interdecades	Duration (d/10a)	Frequency (n/10a)	Intensity (°C/10a)
1962–1970	−1.61	—	2.02
1971–1980	1.76	−0.49	0.56
1981–1990	−6.83	−0.79	−3.21
1991–2000	4.47	0.15	1.26
2001–2010	1.46	0.1	0.2
2011–2020	1.74	0.2	0.1

In terms of spatial distribution, the duration of high-temperature heatwaves in Hexi Oasis showed a gradually decreasing trend from northwest to southeast. The northwestern regions (Su Bei Mongolian Autonomous County, Guazhou County and Yumen City) are primary high-value areas with duration of heatwaves above nine days. For the southeastern (Minqin County, Gulang County, and Jingtai County) and the central (Jinta County) regions, the duration of heatwaves is 6–7 days, while that in the remaining regions is 7–9 days (Figure 3a). As for the frequency of heatwaves in Hexi Oasis, the average annual value is in the range of about 1.07–1.48 times. The spatial distribution of high-value areas of frequency were basically consistent with that of duration, located at Minqin, Jinchuan, Liangzhou, Tianzhu, and Gulang counties in the southeastern, and Ganzhou and Minle counties in the central region, and the low-value areas were mainly in Tianzhu County (Figure 3b). The intensity of heatwaves in the study area exhibits an increasing trend from northwest to southeast within the range from 5.4 to 6.7 °C. Minqin, Jinchuan, Liangzhou, Tianzhu, and Gulang counties in the southeastern, and Ganzhou and Minle counties in the central of the oasis are high-values areas with heatwave intensities ranging from 6.5 to 6.7 °C, while the low-value areas were mainly in Tianzhu County with intensity below 5.9 °C (Figure 3c). The above result indicates that in the last 59a, the southeastern part of the oasis has experienced more intense warming during the heatwave while the western part has undergone relatively modest changes.

As shown by Figure 3d, there is an increasing trend in the variation rate of heatwave duration from southeast to northwest in the last 59a. The high-value areas with a growing rate of 1.5 d/10a were mainly located in Ganzhou District, Minle County and Sunan Yugu Autonomous County. The low-value areas are distributed in Jinta County and Yumen City in the north as well as Minqin County in the southeast, where there is a clear trend toward shorter heatwave duration. Approximately 87.5% of the regions showed an increasing trend (passing the 95% significance test), which is mainly in the central and western parts of the oasis. The remaining 12.5% regions with an opposite trend (passing the 95% significance test) were mainly located in the northern and southeastern parts of the oasis (Figure 3d). The spatial distribution of variation rate of frequency is similar with that of duration, in that the high-value area shows an eastward trend while the low-value area basically does not change significantly. Approximately 71.9% of the regions showed an increasing trend in the frequency variation rate, while the remaining 28.1% of regions exhibit a decreasing trend, mainly distributed in the northern and southeastern part of the oasis (Figure 3e). For the intensity of heatwave, the variation rate gradually increased from northwest to southeast. Minqin County is the region with the most significant increase in the intensity of heatwaves with a growth rate of 0.10 °C/10a. Guazhou County, Yumen City, and Subei Mongolian Autonomous County in the west and Jinta County in the north of the oasis are the regions with decreasing trend (−0.11 °C/10a) in variation rate of heatwave intensity. The southeastern and northern areas of the oasis are the regions with increasing intensity of heatwave, accounting for approximately 77.1% of the total area of the Oasis, and the remaining regions exhibit a decreasing trend in the intensity of heatwaves (Figure 3f).

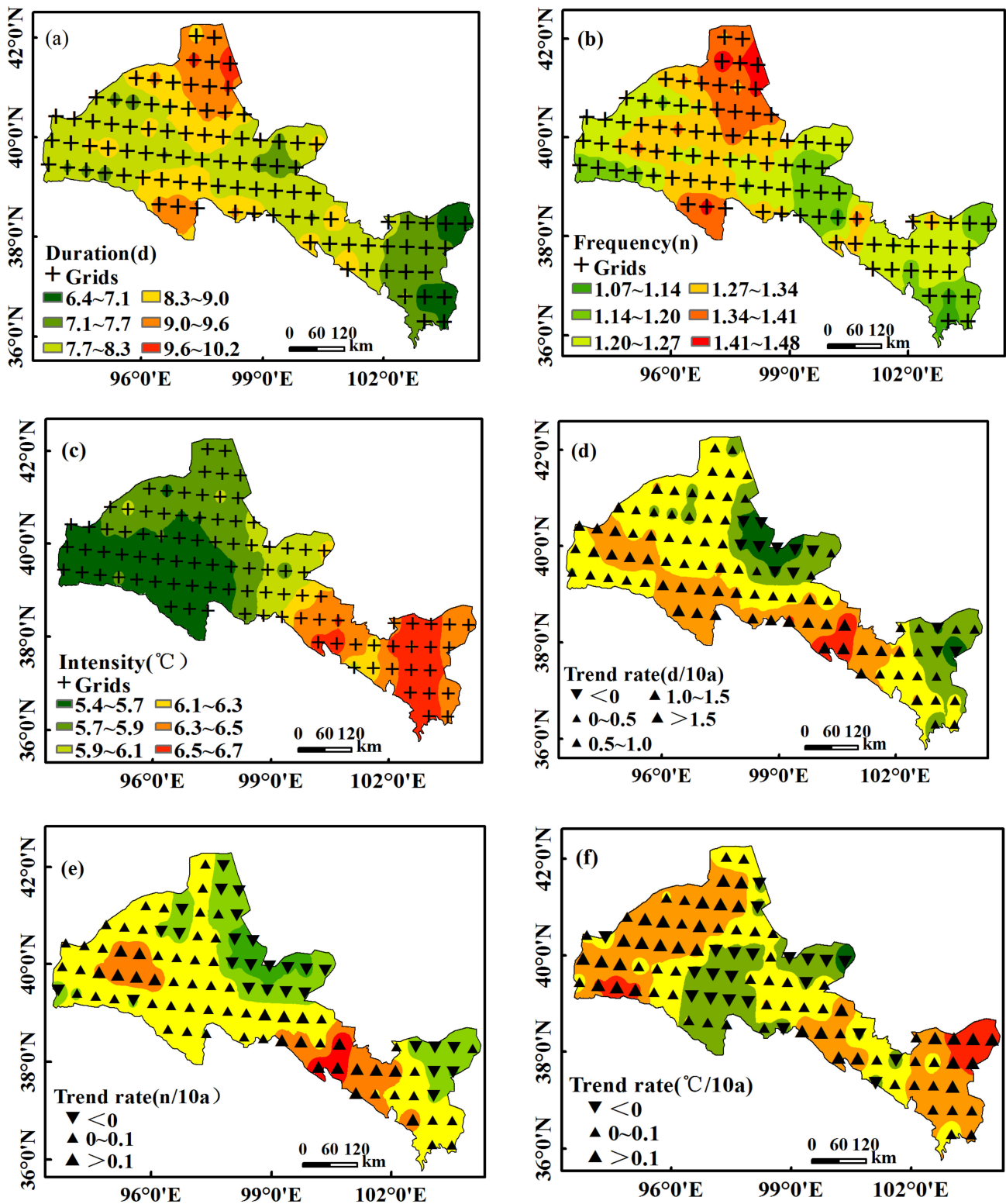


Figure 3. Spatial variation of duration (a), frequency (b) and intensity (c) as well as the tendency rates of duration (d), frequency (e) and intensity (f) of high-temperature heatwaves in Hexi Oasis.

3.2. Mutation Analysis and Cycle Analysis of the Recent 59a High-Temperature Heatwave in Hexi Oasis

In this study, the Mann–Kendall test was used to analyze the mutation of heatwaves in Hexi Oasis from 1962 to 2020 with a subsequence length of 3a and a significance level of $\alpha = 0.01$ and $U\alpha = \pm 2.56$. The results show that there are four intersections of UF and UB

curves for the analysis of mutation in the duration of heatwave over the past 59a, which are 1965, 2003, 2005, and 2009. In 2009, the year with the most obvious mutation, the average duration of heatwave before and after the mutation was 6.4 d and 8.1 d, respectively, gives a significant increase in the number of days (Figure 4a). Meanwhile, the analysis of mutation in the frequency of heatwaves shows that there is no intersection between UF and UB curves (Figure 4b), indicating that the frequency of heatwaves in Hexi Oasis has remained stable in the last 59a. The analysis of the mutation in the intensity of heatwave shows there are four intersections of the UF and UB curves, in 1989, 1992, 2014, and 2016. As evident from Figure 4c, the mutation in 1992 was the most significant, with intensities of 5.5 °C and 5.6 °C before and after the mutation. Based on Figure 4, it can be concluded that the mutation in the duration of heatwaves occurred earliest and was more sensitive to climate change.

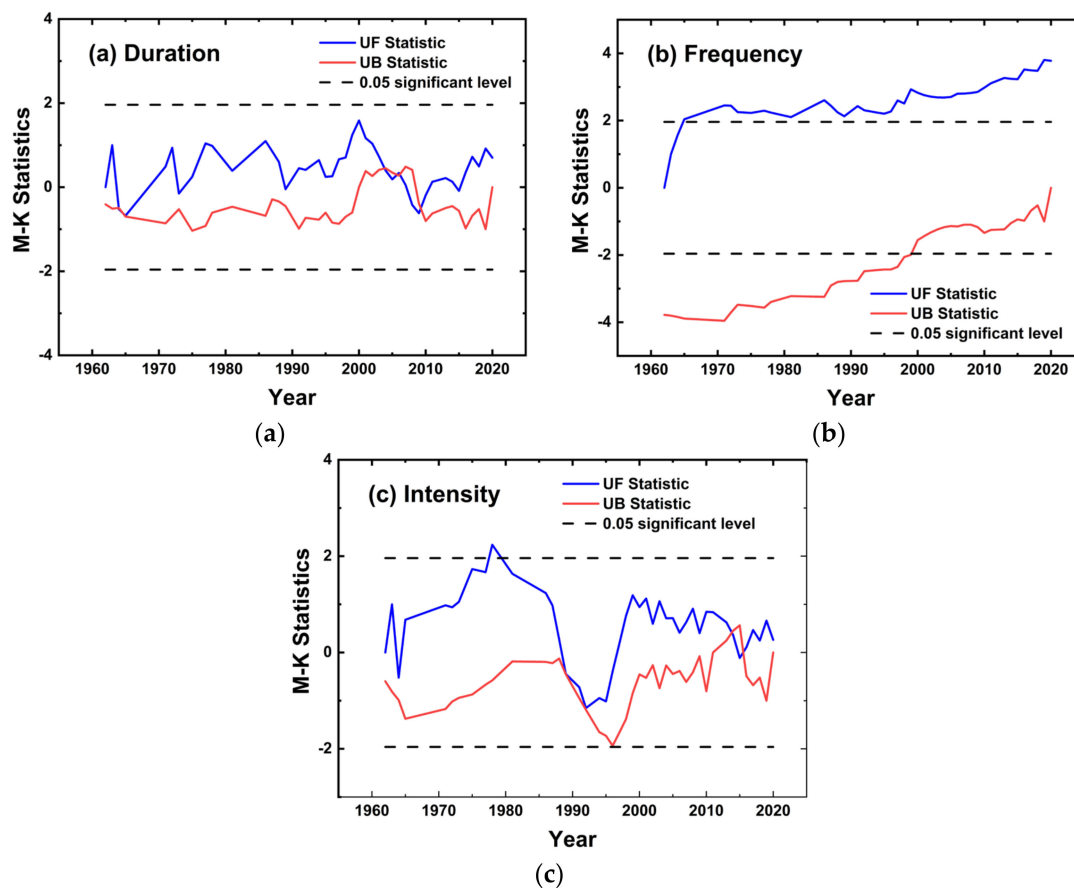


Figure 4. Mutation analysis of duration (a), frequency (b) and intensity (c) of heatwaves in Hexi Oasis (UF and UB are the critical values corresponding to ± 1.96 at the 0.05 significance level respectively).

The Fourier power spectrum analysis was used to analyze the cycle of the high-temperature heatwaves in Hexi Oasis, and the red noise was used to analyze the significance. Overall, there is a significant short-period characteristic of the heatwave in Hexi Oasis. Among them, there are cycles of 2.6a and 7.2a for the duration (Figure 5a,b), 2.8a and 7.6a for the frequency (Figure 5c,d), and 2.6a for the intensity of heatwaves (Figure 5e,f). The duration, frequency, and intensity of heatwaves in Hexi Oasis exceeds the 95% confidence level. The cycles of the heatwave characteristics in Hexi Oasis are basically consistent with those of atmospheric circulation 2–4a and El Niño 2–7a, indicating that the heatwave is mainly influenced by the above events [27]. However, it should be noted that the eastern and central El Niño have different effects on heatwave events in China. There is a decreasing trend of the frequency of heatwave events in northeastern China at eastern

El Niño years, while in central El Niño years there is a decrease of frequency of heatwave events in northeastern China [28,29].

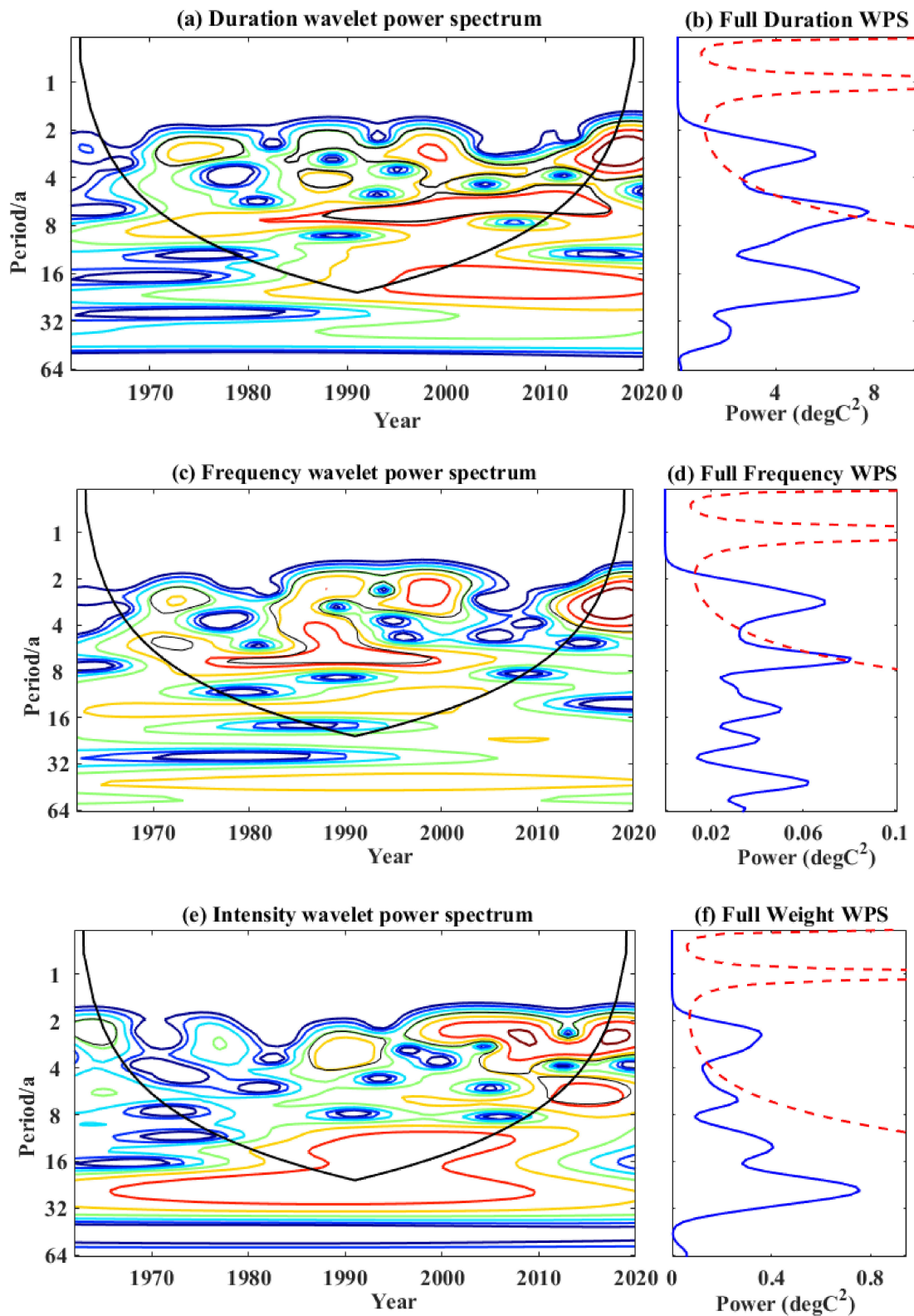


Figure 5. Wavelet power spectrum analysis of duration (a,b), frequency (c,d) and intensity (e,f) of heatwaves in Hexi Oasis.

3.3. Correlation Analysis of Atmospheric Circulation and WPSHP of the Heatwaves in Hexi Oasis for Nearly 59 Years

Generally, atmospheric circulation is the dominant factor causing various weather conditions and is thus closely related to the occurrence of various extreme climate events [30–32]. Therefore, the present study explores the factors influencing the variation of heatwaves in Hexi Oasis from both natural and human aspects. APVAI, APVII, EAT, TPI, and AO were selected as natural factor indicators, and CDE (annual data) was chosen as an anthropogenic factor indicator. The mean values of each indicator from June to September were correlated with the duration, frequency, and intensity of heatwaves to determine the influencing factors, as shown in Table 2.

Table 2. Correlation between the influencing factors and the characterizations of heatwaves in Hexi Oasis.

Atmospheric Circulation Factors	APVAI	APVII	EAT	TPI	AO	CDE
Duration	−0.288 *	−0.111	0.300 *	0.310 *	−0.013	0.280 *
Frequency	−0.211	−0.076	0.252 *	0.245	−0.074	0.229
Intensity	−0.246	−0.046	0.338 **	0.235	−0.020	0.277 *

Note: *, ** indicate the values passed the significant tests at the 95% and 99% confidence intervals, respectively.

From Table 2, one can observe that the heatwave is mainly influenced by APVAI, EAT, TPI, and CDE, which is consistent with the wavelet power spectrum analyzation. When the APVAI value is large, the duration of heatwave is shortened, the frequency is reduced, and the intensity is decreased. There was a relatively high correlation between EAT and the duration, frequency, and intensity of heatwave, especially a significant correlation with intensity which is about 0.338 ($p \leq 0.01$). In addition, there is also a significant correlation between TPI and the duration of heatwave. This is mainly related to the dynamical and thermal effects of the Qinghai-Tibet Plateau, where in winter, due to the branching effect of the plateau, a part of the cold air enters southern Xinjiang from the east while the rest goes south along the Hexi Corridor, which in turn affects the characterizations of heatwaves [33]. Additionally, both the duration and intensity exhibit a high correlation with CDE since the excessive CO₂ emissions are the main cause of global warming, which further demonstrates that the characterization of heatwaves in Hexi Oasis are sensitive to the climate change.

Previous studies have shown that the summer weather in Hexi Oasis is mainly influenced by the West Pacific Subtropical High Pressure (WPSHP). To further investigate the influence of WPSHP on the variability characteristics of heatwaves, regression models were developed.

$$Y1 = -0.19X1 + 0.07X2 + 0.12X3 - 0.08X4 + 14.19 \tag{4}$$

$$Y2 = -0.03X1 + 0.01X2 + 0.01X3 - 0.01X4 + 3.49 \tag{5}$$

$$Y3 = -0.11X1 + 0.04X2 + 0.06X3 - 0.09X4 + 16.05 \tag{6}$$

where Y1, Y2, and Y3 indicate the duration, frequency, and intensity of heatwaves, respectively; X1, X2, X3, and X4 are WPSHA, WPSHI, WPSHRPI, and WPSHNBP, respectively. The results show that the duration of heatwaves increased most significantly with the increase of WPSHA and WPSHRPI. For example, for every 10 m² increase in WPSHA, the duration of heatwave was shortened by 1.9 days, the frequency was reduced by 0.3 times, and the intensity was reduced by 1.1 °C. For every 10 °C increase in WPSHI, the duration is extended by 0.7 days, the frequency increases by 0.1 times, and the intensity increases by 0.4 °C. For every 10° shift of WPSHRPI to the north, the duration of heatwave is shortened by 1.2 days, the frequency is reduced by 0.1 times, and the intensity is reduced by 0.6 °C. For every 10° shift of WPSHNBP to the north, the duration of heatwave is shortened by 0.8 days, the frequency is reduced by 0.1 times, and the intensity is reduced by 0.9 °C. Comparing the above results, it is concluded that the influence of WPSHA on the heatwave events in Hexi Oasis was significantly greater than that of WPSHI, WPSHRPI and

WPSHNBP. In addition, the duration of heatwave was more significantly influenced by the WPSHP than the frequency and intensity. Meanwhile, in this study, the years with stronger and weaker heatwaves were defined by being 1.3 times higher or lower than the average, identifying 1977, 1986, 1999, 2016, and 2019 as years with strong heatwave activity, while 1964, 1989, 2009, 2015, and 2020 as years with weak heatwave activity. In years with strong heatwave activity, there is a remarkable increase of the area of WPSHP, and conversely, the area of WPSHP is rather low at years with weak heatwave activity [28,29,34].

Some limitations concerning the present study should be acknowledged. For example, it is generally accepted that besides the atmospheric anticyclonic circulation as discussed above, the occurrence of heatwaves is also closely related to the changes in sea surface temperature (SST) [35–38]. However, the link between the heatwaves and SST has not been explored in the present work. Further study concerning the influence of SST on the heatwaves in Hexi Oasis will be conducted to construct a coupled sea-air model and clarify the specific process of SST influence on heatwaves. Moreover, soil moisture variation has been increasingly emphasized in the cause and prediction of heatwaves [39,40], and the influence of land-air interaction on high-temperature heatwaves in the Hexi Oasis also deserves a further study with a climate model for future scenario prediction [41,42], so as to provide a theoretical basis for the forecast of high-temperature heatwaves. Additionally, it has been proven that the intensity of heatwaves in eastern China is ~2–4 times higher during drought conditions than in average conditions [4]. Thus, the combined effects of heatwave and drought on human society and crop production in Hexi Oasis and northwestern China should also be studied further in the future.

4. Summary and Conclusions

- (1) In this study, the spatial and temporal variations of high-temperature heatwave in Hexi Oasis are investigated using daily gridded maximum temperature data. The results show that the heatwaves in Hexi Oasis exhibit a trend of prolonged duration, increased frequency, and reduced intensity, and the northwestern part of the oasis is the region where heatwaves are more frequent and long-lasting. In addition, the duration of heatwaves increased significantly in the 1990s. For the spatial distribution, the duration and frequency of heatwaves decreased gradually from northwest to southeast. The northwestern parts of Hexi oasis, such as Subei Mongol Autonomous County, Guazhou County, and Yumen City, are the regions with the longest duration and most frequent heatwaves. In contrast, the southeastern part is the region with the highest intensity of heatwaves.
- (2) Mutation analysis shows that the mutation of duration and intensity of heatwaves occurred in 2009 and 1992, respectively, while the frequency did not change notably. The earliest mutation of the duration of heatwaves indicates it is most sensitive to climate change. Moreover, the variation in heatwave is characterized by short cycles, in which there are cycles of 2.6a and 7.2a for duration, 2.8a and 7.6a for frequency, and 2.6a for intensity. This agrees well with the cycles of atmospheric circulation and El Niño, indicating which have obvious influences on the heatwaves.
- (3) Analyzation of the influencing factors shows that APVAI, EAT, TPI, and CDE are the main driving factors affecting the variation of heatwaves in Hexi Oasis. Additionally, the index of WPSHA increases significantly in years with strong heatwave activity. On the contrary, the WPSHA shrinks significantly in years with weak heatwave activity, while the westward extension and eastward shift of the WPSHP have no obvious influence on the heatwave in Hexi Oasis.

Author Contributions: All authors contributed to the study conception and design. Data collection and analysis were performed by J.L. and H.W. The draft of the manuscript was written by J.L., P.L. commented on it for its improvement. All authors have read and agreed to the published version of the manuscript.

Funding: This work was financially jointly supported by the Youth Science and Technology Fund Project of Gansu Provincial Science and Technology Department (20JR10RA493) and the Project of Gansu Provincial Key Laboratory for Environmental Pollution prediction and Control (kleppc-2019-01).

Institutional Review Board Statement: Not applicable.

Informed Consent Statement: Not applicable.

Data Availability Statement: The in-situ temperature data were provided by the China Meteorology Administration (CMA) "<http://data.cma.cn/>" (accessed on 1 January 2023)". The elevation data were SRTM with 30 m resolution from the geospatial data cloud "<http://www.gscloud.cn>" (accessed on 1 January 2023)". The data are not available to the public due to legal constraints on the data's availability.

Conflicts of Interest: The authors declare no conflict of interest.

Abbreviations

Abbreviations	Professional Terms
M-K	Mann-Kendall
EAT	East Asia Major Trough
TPI	Qinghai-Tibetan Plateau Index
CDE	Carbon Dioxide Emissions
APVAI	Asian Zone Polar Vortex Area Index
APVII	Asian Polar Vortex Intensity Index
AO	Arctic Oscillation Index
WPSHA	Western Pacific Sub-High Area Index
WPSHI	Western Pacific Sub-High Intensity Index
WPSHRPI	Western Pacific Sub-High Ridge Position Index
WPSHNBP	and Western Pacific Sub-High Northern Boundary Position Index
WPSHP	West Pacific Subtropical High Pressure
SST	sea surface temperature

References

- IPCC. Climate Change 2021: The Physical Science Basis. In *Contribution of Working Group I to the Sixth Assessment Report of the Intergovernmental Panel on Climate Change*; Masson-Delmotte, V., Zhai, P., Pirani, A., Connors, S.L., Péan, C., Berger, S., Caud, N., Chen, Y., Goldfarb, L., Gomis, M.I., et al., Eds.; Cambridge University Press: Cambridge, UK, 2021.
- Chen, H.J.; Zhao, L.; Dong, W.; Cheng, L.L.; Cai, W.J.; Yang, J.; Bao, J.Z.; Liang, X.Z.; Shakoob, H.; Gong, P.; et al. Spatiotemporal variation of mortality burden attributable to heatwaves in China, 1979–2020. *Sci. Bull.* **2022**, *67*, 1340–1344. [[CrossRef](#)] [[PubMed](#)]
- Wang, S.S.; Yuan, X.; Wu, R.G. Attribution of the persistent spring-summer hot and dry extremes over northeast china in 2017. *Bull. Am. Meteorol. Soc.* **2019**, *100*, S85–S89. [[CrossRef](#)]
- Kong, Q.Q.; Guerreiro, S.B.; Blenkinsop, S.; Li, X.F.; Fowler, H.J. Increases in summertime concurrent drought and heatwave in Eastern China. *Weather Clim. Extrem.* **2020**, *28*, 100242. [[CrossRef](#)]
- Hobday, A.J.; Alexander, L.V.; Perkins, S.E.; Smale, D.A.; Straub, S.C.; Oliver, E.C.J.; Benthuisen, J.A.; Burrows, M.T.; Donat, M.G.; Feng, M.; et al. A hierarchical approach to defining marine heatwaves. *Prog. Oceanogr.* **2016**, *141*, 227–238. [[CrossRef](#)]
- Zhang, H.F.; Liu, L.X.; Zeng, Y.; Liu, M.M.; Bi, J.; Ji, J.S. Effect of heatwaves and greenness on mortality among Chinese older adults. *Environ. Pollut.* **2021**, *290*, 118009. [[CrossRef](#)]
- Scherrer, S.C.; Fischer, E.M.; Posselt, R.; Liniger, M.A.; Croci-Maspoli, M.; Knutti, R. Emerging trends in heavy precipitation and hot temperature extremes in Switzerland. *J. Geophys. Res.-Atmos.* **2016**, *121*, 2626–2637. [[CrossRef](#)]
- Garca-Herrera, R.; Diaz, J.; Trigo, R.M.; Fischer, E.M. A Review of the European Summer Heat Wave of 2003. *Crit. Rev. Environ. Sci. Technol.* **2010**, *40*, 267–306. [[CrossRef](#)]
- Fouillet, A.; Rey, G.; Laurent, F.; Pavillon, G.; Bellec, S.; Guihenneuc-Jouyau, C.; Clavel, J.; Jouglu, E.; Hémon, D. Excess mortality related to the August 2003 heat wave in France. *Int. Arch. Occup. Environ. Health* **2006**, *80*, 16–24. [[CrossRef](#)]
- Habeeb, D.; Vargo, J.; Stone, B., Jr. Rising heat wave trends in large US cities. *Nat. Hazards* **2015**, *76*, 1651–1665. [[CrossRef](#)]
- Dole, R.; Hoerling, M.; Perlwitz, J.; Eischeid, J.; Pegion, P.; Zhang, T.; Quan, X.W.; Xu, T.Y.; Murray, D. Was there a basis for anticipating the 2010 Russian heat wave? *Geophys. Res. Lett.* **2011**, *38*, L06702. [[CrossRef](#)]
- Jia, J.; Hu, Z.Y. Spatial and temporal features and trend of different level heat waves over China. *Prog. Geogr.* **2017**, *32*, 546–559. (In Chinese) [[CrossRef](#)]
- Shen, H.J.; You, Q.L.; Wang, P.L.; Kong, L. Analysis on heat waves variation features in China during 1961–2014. *Sci. Meteorol. Sin.* **2018**, *38*, 28–36. (In Chinese) [[CrossRef](#)]

14. Zhang, Y.; Zhang, L.; Wang, S.P.; Feng, J.Y. Drought Events and Its Influence in Summer of 2017 in China. *Arid. Meteorol.* **2017**, *35*, 899–905. (In Chinese) [[CrossRef](#)]
15. Yang, J.; Yin, P.; Sun, J.M.; Wang, B.G.; Zhou, M.G.; Li, M.M.; Tong, S.L.; Meng, B.H.; Guo, Y.M.; Liu, Q.Y. Heatwave and mortality in 31 major Chinese cities: Definition, vulnerability and implications. *Sci. Total. Environ.* **2019**, *649*, 695–702. [[CrossRef](#)]
16. Zhang, Y.Q.; Feng, R.J.; Wu, R.; Zhong, P.R.; Tan, X.D.; Wu, K.; Ma, L. Global climate change: Impact of heat waves under different definitions on daily mortality in Wuhan, China. *Glob. Health Res. Policy* **2017**, *2*, 10. [[CrossRef](#)]
17. Gao, Z.R.; Tian, Q.M.; Liu, X.Y.; Wang, X.F.; Yang, Q.H. Analysis of temperature changes and abrupt changes in the Hexi Corridor in the past 58 years. *Arid. Zone Res.* **2010**, *27*, 194–203. [[CrossRef](#)]
18. Cao, L.G.; Pan, S.M.; Jia, P.H.; Zhuoma, L.C.; Zhao, Y.F.; Zhang, K.X.; Zhang, W. Evolution characteristics of extreme dry and wet events in the Hexi region from 1960 to 2009. *J. Nat. Resour.* **2014**, *29*, 480–489. (In Chinese)
19. Tao, J.H.; Kong, X.W.; Liu, X.W. Analysis of water vapor characteristics of two extreme rainstorm events in the western Hexi Corridor. *Plateau Meteorol.* **2016**, *35*, 107–117. (In Chinese) [[CrossRef](#)]
20. Shen, Y.C.; Wang, J.W.; Wu, G.H.; Han, D.L. *Oasis of China*; Henan University Press: Zhengzhou, China, 2001; pp. 332–338. (In Chinese)
21. Wang, Y.W.; Luo, L.; Zhang, F.; Chen, T.L. Soil Conservation Effect of Haloxylon Ammodendron Bushes in Hexi Oasis-Desert Ecotone. *Acta Polym. Sin.* **2019**, *56*, 749–762. (In Chinese) [[CrossRef](#)]
22. Wang, Y.J.; Liu, X.F.; Zhai, J.Q.; Wang, Y.Y.; Jiang, T. Variation characteristics of extreme precipitation in the Yangtze River Basin under the global warming 1.5 °C and 2.0 °C. *J. Meteorol. Sci.* **2019**, *39*, 540–547.
23. Yao, Y.B.; Liu, J.N.; Zhang, M.; Zhao, J.F.; Li, Q.; Li, D.L.; Li, Y.; Zhang, X.Y. Impact of Climatic Change on the Agriculture in Hexi Oasis and Countermeasures. *Ecol. Environ.* **2020**, *29*, 1499–1506. (In Chinese) [[CrossRef](#)]
24. Liu, S.X.; Zhang, J.; Zhao, J.H. Analysis of abrupt climate change in the last fifty years in Hexi area. *Adv. Earth Sci.* **2007**, *22*, 0066–07.
25. Ye, D.X.; Yin, J.F.; Chen, Z.H.H.; Zheng, Y.F.; Wu, R.J. Spatial and temporal characteristics of summer heat waves in China from 1961 to 2010. *Adv. Clim. Change Res.* **2013**, *9*, 15–20.
26. Wu, J.C.; Zhu, Y.; Liu, Y.; Yin, H.; Yuan, F.; Wang, J. Analysis of spatial and temporal variability of heat waves in China. *Hydrology* **2022**, *42*, 72–77. (In Chinese) [[CrossRef](#)]
27. Zhang, W.X.; Liu, P.X.; Feng, Q.R.; Wang, T.G.; Wang, T.Q. The spatiotemporal responses of *Populus euphratica* to global warming in Chinese oases between 1960 and 2015. *J. Geogr. Sci.* **2018**, *28*, 16. [[CrossRef](#)]
28. Li, Y.; Ma, B.S.; Yang, X.; Zhang, J.Y. Characteristics of summer heat waves in China Mainland and the relationship between Eastern-/Central-Pacific El Niño and heat wave events. *J. Lanzhou Univ. (Nat. Sci.)* **2018**, *54*, 711–720. [[CrossRef](#)]
29. Zhou, Y.F.; Wu, Z.W. Possible impacts of mega-El Nino/Southern Oscillation and Atlantic Multidecadal Oscillation on Eurasian heatwave frequency variability. *Q. J. R. Meteorol. Soc.* **2016**, *142*, 1647–1661. [[CrossRef](#)]
30. Wang, Y. *Temporal and Spatial Characteristics of Temperature of the Phenological Solar Term and Its Impact Factors in Northwest Oasis during 1960~2013*; Northwest Normal University: Lanzhou, China, 2016. (In Chinese)
31. Zhang, G.W.; Zeng, G.; Li, C.; Yang, X.Y. Impact of PDO and AMO on interdecadal variability in extreme high temperatures in North China over the most recent 40-year period. *Clim. Dyn.* **2020**, *54*, 3003–3020. [[CrossRef](#)]
32. Zhou, M.Z.; Wang, H.J.; Hou, Z.G. The Influence of Heat Stress on Maize Yield and Its Association with Atmospheric General Circulation and Sea Surface Temperature. *Clim. Environ. Res.* **2017**, *22*, 134–148. (In Chinese) [[CrossRef](#)]
33. Chen, L.; Wang, S.G.; Shang, K.Z.; Yang, D.B. Atmospheric circulation anomalies of large-scale extreme high temperature events in northwest China. *J. Desert Res.* **2011**, *31*, 1052–1058. (In Chinese)
34. Qi, L.; Zhou, T.; Mao, H.; Fu, C. Decadal variations in the relationship between the western pacific subtropical high and summer heat waves in east China. *J. Clim.* **2019**, *32*, 1627–1640. [[CrossRef](#)]
35. Chen, X.; Zhou, T. Relative contributions of external SST forcing and internal atmospheric variability to July-August heat waves over the Yangtze River valley. *Clim. Dyn.* **2018**, *51*, 4403–4419. [[CrossRef](#)]
36. Deng, K.Q.; Yang, S.; Ting, M.F.; Zhao, P.; Wang, Z.Y. Dominant Modes of China Summer Heat Waves Driven by Global Sea Surface Temperature and Atmospheric Internal Variability. *J. Clim.* **2019**, *32*, 3761–3775. [[CrossRef](#)]
37. Freychet, N.; Tett, S.; Wang, J.; Hegerl, G. Summer heat waves over Eastern China: Dynamical processes and trend attribution. *Environ. Res. Lett.* **2017**, *12*, 024015. [[CrossRef](#)]
38. Zhao, Y.C.; Zhao, X.F.; Liu, L.L. Spatial pattern analysis on human health risk of heatwave in xiamen city. *J. Geo-Inf. Sci.* **2016**, *18*, 1094–1102. [[CrossRef](#)]
39. Koster, R.D.; Chang, Y.H.; Wang, H.L.; Schubert, S.D. Impacts of Local Soil Moisture Anomalies on the Atmospheric Circulation and on Remote Surface Meteorological Fields during Boreal Summer: A Comprehensive Analysis over North America. *J. Clim.* **2016**, *29*, 7345–7364. [[CrossRef](#)]
40. Vogel, M.M.; Orth, R.; Cheruy, F.; Hagemann, S.; Lorenz, R.; Hurk, B.J.J.M.; Seneviratne, S.I. Regional amplification of projected changes in extreme temperatures strongly controlled by soil moisture temperature feedbacks. *Geophys. Res. Lett.* **2017**, *44*, 1511–1519. [[CrossRef](#)]

41. Liu, L.; Liu, P.X.; Zhang, W.X.; Si, W.Y.; Qiao, X.M. Characteristics of extreme warm events changes in Xinjiang from 1961–2017 and their future scenario prediction. *Arid. Zone Res.* **2021**, *38*, 1590–1600. [[CrossRef](#)]
42. Xu, H.R.; Zhang, G.W. Comparison of Relative and Absolute Heatwaves in Eastern China: Observations, Simulations and Future Projections. *Atmosphere* **2022**, *13*, 649. [[CrossRef](#)]

Disclaimer/Publisher’s Note: The statements, opinions and data contained in all publications are solely those of the individual author(s) and contributor(s) and not of MDPI and/or the editor(s). MDPI and/or the editor(s) disclaim responsibility for any injury to people or property resulting from any ideas, methods, instructions or products referred to in the content.